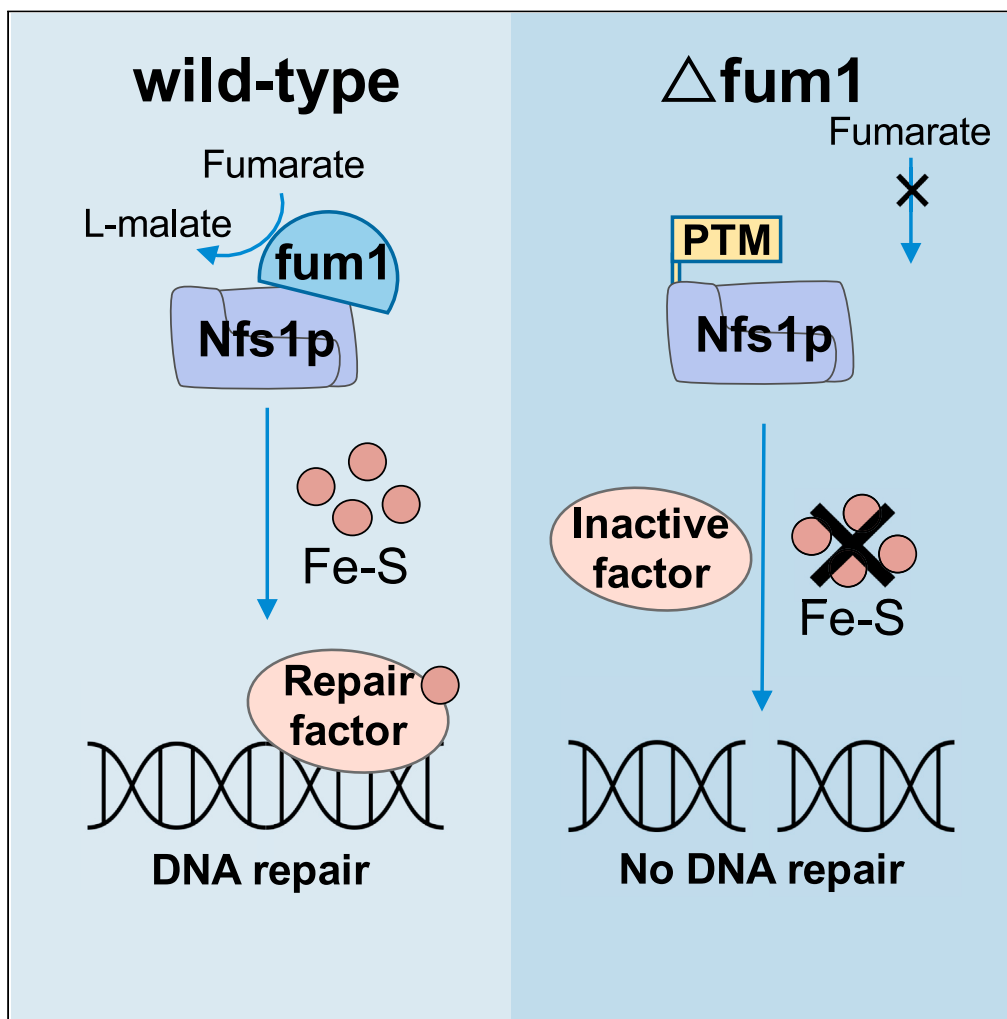**Article**

Fumarase affects the deoxyribonucleic acid damage response by protecting the mitochondrial desulfurase Nfs1p from modification and inactivation

Joyce Yip, Suqing Wang, Jasper Tan, ..., Ofri Karmon, Ophry Pines, Norbert Lehming

ophryp@ekmd.huji.ac.il (O.P.)
micln@nus.edu.sg (N.L.)

Highlights

Overexpression of Nfs1p restores DNA repair in yeast cells lacking fumarase

Nfs1p is required for DNA repair as it provides DNA repair factors with Fe–S clusters

Nfs1p accumulates inactivating modifications in yeast cells lacking fumarase

Fumarase aids DNA repair by protecting Nfs1p from inactivating modifications

Article

Fumarase affects the deoxyribonucleic acid damage response by protecting the mitochondrial desulfurase Nfs1p from modification and inactivation

Joyce Yip,[1,4] Suqing Wang,[1,4] Jasper Tan,[1] Teck Kwang Lim,[2] Qingsong Lin,[2] Zhang Yu,[3] Ofri Karmon,[3] Ophry Pines,[3,*] and Norbert Lehming[1,5,*]

SUMMARY

The Krebs cycle enzyme fumarase, which has been identified as a tumor suppressor, is involved in the deoxyribonucleic acid (DNA) damage response (DDR) in human, yeast, and bacterial cells. We have found that the overexpression of the cysteine desulfurase Nfs1p restores DNA repair in fumarase-deficient yeast cells. Nfs1p accumulates inactivating post-translational modifications in yeast cells lacking fumarase under conditions of DNA damage. Our model is that in addition to metabolic signaling of the DDR in the nucleus, fumarase affects the DDR by protecting the desulfurase Nfs1p in mitochondria from modification and inactivation. Fumarase performs this protection by directly binding to Nfs1p in mitochondria and enabling, the maintenance, via metabolism, of a non-oxidizing environment in mitochondria. Nfs1p is required for the formation of Fe–S clusters, which are essential cofactors for DNA repair enzymes. Thus, we propose that the overexpression of Nfs1p overcomes the lack of fumarase by enhancing the activity of DNA repair enzymes.

INTRODUCTION

Fumarase converts fumarate to L-malate in mitochondria as part of the tricarboxylic acid (TCA) cycle (Krebs et al., 1938), while the cytosolic form of fumarase enters the nucleus of human and yeast cells under conditions of deoxyribonucleic acid (DNA) damage and there it converts L-malate to fumarate (Yogev et al., 2010; Jiang et al., 2015). Nuclear fumarate aids DNA repair and when cytosolic fumarase is absent from cells, the DNA damage response (DDR) is deficient (Yogev et al., 2010). The catalytic activity of fumarase is required for its role in the DDR and fumarate restores the DDR in fumarase-deficient yeast cells (Yogev et al., 2010). The inability to repair damaged DNA is a hallmark of cancer (Hanahan and Weinberg, 2011), and a study with patients suffering from hereditary leiomyomatosis and renal cell cancer (HLRCC) identified fumarase as a tumor suppressor (Tomlinson et al., 2002), suggesting that HLRCC could be caused by the DNA repair defect of cells lacking fumarase. The absence of functional fumarase leads to the accumulation of fumarate in the cell (Yang et al., 2014). Fumarase and other TCA-related intermediates metabolically signal the DDR in human, yeast, and bacterial cells (Yogev et al., 2010; Singer et al., 2017; Wang et al., 2020; Silas et al., 2021). In the context of this study, it is worth mentioning that the reaction between fumarate and cysteine residues of proteins can lead to a post-translational modification known as succination (Blatnik et al., 2008).

Fe–S clusters act as crucial cofactors in proteins of the electron transport chain and TCA cycle, which includes enzymes such as complex III, succinate dehydrogenase, and aconitase, serving as an electron carrier and partaking in redox reactions (Barros and McStay, 2020). In addition to many other proteins, the Fe–S clusters also serve as co-factors for DNA repair enzymes such as XPD, RTEL1, and DNA polymerase, suggesting that Fe–S clusters also play a crucial role in DNA repair (Netz et al., 2011; Fuss et al., 2015).

Nfs1p is an essential cysteine desulfurase that is required for the generation of Fe–S clusters (Kispal et al., 1999). During Fe–S biogenesis, Nfs1p removes the sulfur group from free cysteine, resulting in the formation of alanine during the process (Mühlenhoff et al., 2004). This sulfur group is then passed on to Isu1p in *Saccharomyces cerevisiae* or ISCUp in humans, where the Fe–S cluster is assembled (Cardenas-Rodriguez et al., 2018). Intriguingly, a heterozygous mutation of *NFS1* was found to cause genetic instability in a yeast

Figure 1. Overexpression of Nfs1p restores DNA repair in cells lacking fumarase

(A) Overexpression of Nfs1p from the multi-copy vector YEp13 under the control of its own promoter restored growth of diploid *BY4743ΔWΔfum1* cells on plates containing 360mM HU: Cells of the indicated genotype were 10-fold serially diluted, spotted onto the depicted plates, and incubated for 12 days at 28°C.

(B) Restoration of DNA repair requires mitochondrial localization of Nfs1p: Overexpression of Nfs1p, but not Nfs1p lacking its mitochondrial targeting signal MTS, from the multi-copy vector PADNX under the control of the strong *ADH1*

Figure 1. *Continued*

promoter restored growth of haploid *BY4742ΔWΔfum1* cells on plates containing 300mM HU. Cells of the indicated genotype were 10-fold serially diluted, spotted onto the depicted plates, and incubated for six days at 28°C.

(C) Cytosolic Fum1p interacts with cytosolic Nfs1p in the split-Ub assay in vivo: Cells of the indicated genotype were 10-fold serially diluted, spotted onto the depicted plates, and incubated for six days at 28°C. Nub-Fum1ΔMTSp was expressed from the *ADH1* promoter, while Nub-Nfs1ΔMTS was expressed from the *NFS1* promoter. Fum1ΔMTS-Cub-RUra3p was expressed from the *FUM1* promoter and Nfs1ΔMTS-Cub-RUra3p was expressed from the *NFS1* promoter. The protein–protein interaction between Fum1p and Nfs1p in the cytosol is indicated by the absence of growth on the plate lacking uracil.

(D) Fumarase interacts with Nfs1p in a GST pull-down assay in vitro: GST and GST-Nfs1ΔMTSp were purified with glutathione beads in the presence of H_6-HA-Fum1ΔMTSp. Co-precipitated H_6-HA-Fum1ΔMTSp was detected with an anti-HA antibody.

model of cancer evolution (Coelho et al., 2019) and lung tumors require a high expression of NFS1 to prevent ferroptosis (Alvarez et al., 2017). We have found here that the overexpression of Nfs1p restored DNA repair in yeast cells lacking fumarase. Mass spectrometry (MS) demonstrates that Nfs1p accumulates inactivating post-translational modifications in yeast cells lacking fumarase under conditions of DNA damage.

RESULTS

Nfs1p overexpression complements the DNA damage response defect of cells lacking fumarase

Yeast cells lacking fumarase have a DNA repair defect, and they are unable to grow on plates containing high concentrations of the DNA-damaging agent hydroxyurea (HU). We screened a library of *S. cerevisiae* genomic DNA fragments cloned into the *LEU2*-marked multi-copy plasmid YEp13 (Nasmyth and Reed, 1980) for suppressors of this DNA repair defect. Diploid *BY4743ΔWΔfum1* (*Δfum1*) cells were transformed with the library and approximately 100,000 transformants were spread onto plates lacking leucine and containing 360mM HU. The plasmid DNA of colonies that grew on these plates was isolated and re-transformed into *Δfum1* cells, which were then retested for growth on HU plates. The genomic DNA fragments of confirmed plasmids were sequenced and the suppressor genes were identified by sub-cloning them into the *LEU2*-marked multi-copy plasmid YEplac181. Figure 1A shows that the cysteine desulfurase Nfs1p was isolated as a multi-copy suppressor by its ability to restore the growth of *Δfum1* cells on an HU plate (compare lines 1 and 2 with lines 3 and 4 for *Δfum1*). The overexpression of Nfs1p had no effect on the ability of wild-type cells to grow on the HU plate (compare lines 1 and 2 with lines 3 and 4 for *BY4743ΔW*). Importantly, Figures 1B and S1A show that mitochondrial localization of Nfs1p is required, because cells overexpressing Nfs1p lacking a mitochondrial targeting signal (ΔMTS) under the control of a strong promoter failed to restore growth on HU plates (compare lines 3 and 4 with lines 5 and 6 in both figures).

Nfs1p and fumarase interact

A split-ubiquitin screen with cytosolic fumarase as bait identified Nfs1(155-268)p as a novel Fum1p protein–protein interaction partner (Figure S2, lines 3 and 4). Wild-type *BY4743ΔW* cells expressing a fusion of cytosolic fumarase to the C-terminal half of ubiquitin (Cub) extended by the Ura3p enzyme whose first amino acid been replaced by an arginine (Fum1ΔMTS-Cub-RUra3p) were transformed with a library of plasmids expressing open reading frame fusions of *S. cerevisiae* genomic DNA fragments to the N-terminal half of ubiquitin (Nub) (Laser et al., 2000). Proteins that interact with fumarase bring Nub and Cub into close proximity and RUra3p is cleaved off by the ubiquitin-specific proteases. The enzymes of the N-end rule degrade RUra3p so quickly that the cells become phenotypically uracil auxotroph and resistant to 5-fluoroorotic acid (FOA) (Lehming, 2002). Proteins interacting with cytosolic fumarase under conditions of DNA damage were identified by their ability to confer growth on FOA plates that contained 100mM HU. The in vivo protein–protein interaction of cytosolic fumarase with the cysteine desulfurase Nfs1p together with the finding that the overexpression of Nfs1p compensates for the *fum1* gene deletion, suggests that this interaction protects Nfs1p activity. In order to confirm this understanding, we checked whether full-length Fum1p can interact with full-length Nfs1p. Nub and Cub-RUra3p were fused to both full-length proteins without their mitochondrial targeting signals. Figure 1C shows that the co-expression of Nub-Fum1ΔMTSp and Nfs1ΔMTS-Cub-RUra3p resulted in reduced growth on plates lacking uracil, indicating that both proteins interacted in vivo (compare line 1 with lines 2 and 3). The figure further shows that the same protein–protein interaction was observed when the fusions were swapped (compare line 4 with lines 5 and 6). The growth defect was more pronounced in the presence of HU, suggesting that the protein–protein interaction between Fum1p and Nfs1p was stronger when the cells were grown under conditions
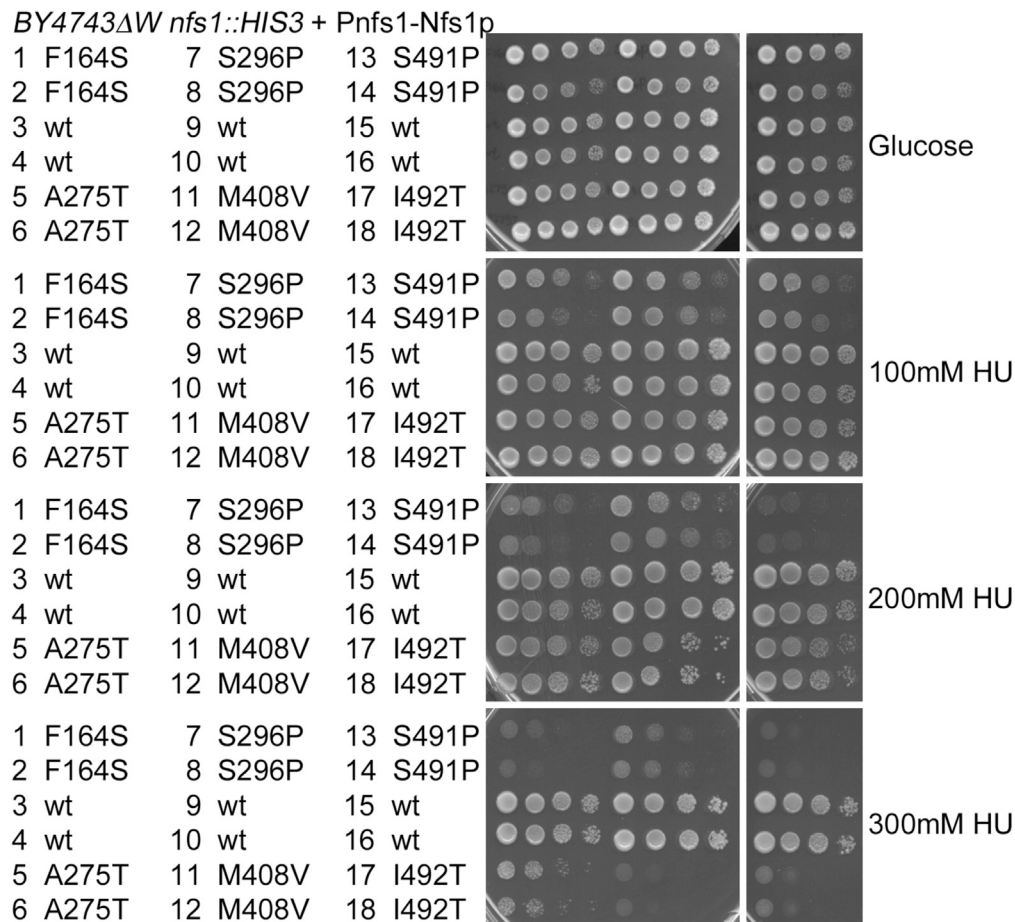
Figure 2. Nfs1p is required for DNA repair

The mutant Nfs1p proteins F164S, A275T, S296P, M408V, S491P, I492T fail to support DNA repair. The ability to support DNA repair is indicated by growth on the HU plates. Cells of the indicated genotype were 10-fold serially diluted, spotted onto the depicted plates, and incubated for six days at 28°C.

of DNA damage. The split-ubiquitin assay demonstrates close proximity of two proteins inside living cells, but not necessarily a direct protein–protein interaction (Lehming, 2002).

To demonstrate that the two proteins interact directly, we fused Nfs1ΔMTSp to GST and Fum1ΔMTSp to six histidines and the hemagglutinin (HA) epitope and expressed both fusions in *Escherichia coli* cells. The anti-GST panels in Figure 1D show that glutathione sepharose pulled down both GST and GST-Nfs1ΔMTSp from an *E. coli* protein extract, while the anti-HA panels in Figure 1D show that GST-Nfs1ΔMTSp, but not GST, co-precipitated H_6-HA-Fum1ΔMTSp, demonstrating that Nfs1p and Fum1p interact directly with each other.

Isolation of specific Nfs1p mutants that are defective in DNA repair

The cysteine desulfurase Nfs1p is required to generate Fe–S clusters, which are essential cofactors for the TCA cycle enzymes aconitase and succinate dehydrogenase, for proteins of the electron transport chain and for DNA repair enzymes like XPD (Rad3p) and DNA polymerase (Netz et al., 2011). *NFS1* is an essential gene, and we were, therefore, unable to test its gene deletion strain for sensitivity to HU. In order to demonstrate that Nfs1p is required for DNA repair, we combined plasmid shuffle with replica plating to isolate HU-sensitive *nfs1* mutants that are evidently unable to repair their damaged DNA. The mutations were identified by DNA sequencing and for plasmids that contained more than one mutation, molecular cloning was used to identify which mutations were functionally relevant (Figure S3). Figure 2 shows that the six Nfs1p mutant proteins such as F164S, A275T, S296P, M408V, S491P, and I492T failed to support

DNA repair, with *nfs1F164S*, *nfs1S296P*, and *nfs1S491P* being more sensitive to HU as compared with the other three *nfs1* mutant strains. The three Nfs1p mutant proteins such as F164S, S296P, and S491P also failed to support respiration (Figure S4B, lines 1, 4, and 9), while the other three Nfs1p mutant proteins such as A275T, M408V, and I492T did support respiration (Figure S4B, lines 3, 7, and 10). Data S1 shows that S491 is conserved in 8 out of 10 species, while the other five residues are completely conserved. The most likely explanation of the DNA repair defect of the *nfs1* mutant strains is that they contain insufficient Fe–S clusters. Aconitase (Aco1p) is proteolytically unstable without its Fe–S cluster (Adam et al., 2006; Bedekovics et al., 2011) and Aco1p disappears from *nfs1F164S* cells upon two hours of growth at 38°C (Figure S5), confirming that Fe–S clusters are limiting in the *nfs1F164S* mutant strain at the non-permissive temperature.

Expression of Nfs1F164Sp is upregulated

Nfs1(F164S)p was chosen for further analysis because F164S was the only mutation in the Fum1p-interacting domain of Nfs1p that we had been able to identify as causing sensitivity to HU. A Western blot with an anti-Nfs1p antibody demonstrated that the Nfs1(F164S)p mutant protein was expressed at higher levels as compared with wild-type Nfs1p (Figure 3B, compare lanes 2 and 3 with lanes 4 and 5), consistent with the hypothesis that the cells compensate for the low amounts of Fe–S clusters by increasing the expression of the *NFS1* gene. Total RNA was isolated from cells expressing Nfs1p wild-type and Nfs1(F164S)p under the control of the *NFS1* promoter. The amount of *NFS1* mRNA relative to *ACT1* mRNA was determined by RT-coupled qPCR. Figure 3C shows that *nfs1F164S* cells expressed approximately 24 times more *NFS1* mRNA as compared with *NFS1* wild-type cells when the cells were grown under normal conditions and approximately 14 times more when the cells were grown under conditions of DNA damage. We overexpressed wild-type Nfs1p and the six Nfs1p mutant proteins under the control of the strong *ACT1* promoter and found that the Nfs1p mutant proteins were now expressed at protein levels comparable to wild-type Nfs1p (Figure 3B, compare lanes 2 to 9), confirming our hypothesis that the difference in Nfs1 expression under the control the *NFS1* promoter was owing to *NFS1* mRNA levels and not Nfs1p protein stability. Cells overexpressing the Nfs1p mutant proteins from the strong *ACT1* promoter were still sensitive to HU, even though some of the phenotypes were less pronounced as compared to Nfs1p expressed from its own promoter (Figure S6, compare panels A and B).

Nfs1(F164S)p is defective for protein interaction with fumarase

The split-ubiquitin screen revealed that Nfsp1p residues 155–268 are sufficient for the interaction with fumarase (Figure S2). F164S was the only mutation in this domain that we had been able to identify as causing sensitivity to HU. We tested full-length cytosolic Nfs1(F164S)p in the split-ubiquitin assay and we found that it was unable to interact with fumarase (Figure 4A), both when it was fused to Nub (lines 5 and 6) and when it was fused to Cub-RUra3p (lines 11 and 12). To confirm this observation in vitro, the Nfs1(F164S)p mutant protein was fused to GST (without MTS) and expressed in *E. coli* cells. The anti-GST panels in Figure 4B show that while GST-Nfs1(F164S)ΔMTSp was expressed at lower protein levels than GST-Nfs1ΔMTSp in *E. coli* cells, glutathione sepharose pulled down both full-length fusions at comparable levels. The ΔC130 truncated GST-Nfs1p fusion, which still contains the fumarase interaction domain, was pulled down at even higher levels for the F164S mutant protein as compared with the wild-type protein. The anti-HA panels in Figure 4B show that the GST-Nfs1(F164S)ΔMTSp mutant protein was able to co-precipitate approximately three times less fumarase as compared to wild-type GST-Nfs1ΔMTSp. As a control, we also tested the effect of the A275T mutation, which is outside of the Nfs1(155–268)p fumarase interaction domain, and we found that the A275T mutation did not decrease the protein interaction of Nfs1 with fumarase. We conclude that Nfs1F164 is required for the interaction with Fum1p.

ISU1 or ISU2 overexpression suppresses the DNA damage sensitivity of nfs1S491P and nfs1I492T

To further our understanding of why the Nfs1p mutant proteins were unable to support DNA repair, we performed multi-copy suppressor screens with the *nfs1F164S* and *nfs1S491P* mutant strains. The strains were transformed with the *LEU2*-marked multi-copy library of *S. cerevisiae* genomic DNA fragments (Nasmyth and Reed, 1980) and approximately 100,000 transformed cells were spread onto plates lacking leucine and containing 300mM HU. The plasmid DNA of colonies that grew on these plates was isolated and retested. The genomic DNA fragments were sequenced and candidate genes were confirmed by sub-cloning them into the multi-copy vector YEplac181. Although we did not obtain suppressors for *nfs1F164S*, we

A

B

C

Figure 3. The Nfs1(F164S)p mutant protein is expressed at protein levels higher than those of wild-type Nfs1p

(A) Cells expressing Nfs1p and its indicated derivatives, from the single-copy vector RS314 under the control of the *NFS1* promoter, were grown in liquid glucose media in the absence [G] or presence of 400 mM HU for two hours [H]. Cells were boiled in SDS loading dye and proteins were separated on 8%PAA gels. Nfs1p was detected with anti-Nfs1p antibody while anti-CPY (Carboxypeptidase Y) was the loading control.

(B) Nfs1p and its indicated derivatives overexpressed from RS314 under the control of the strong *ACT1* promoter were loaded into lanes 6 to 26. Nfs1p and the Nfs1(F164S)p mutant protein expressed from RS314 under the control of the *NFS1* promoter were loaded as a comparison in lanes 2 to 5.

(C) Cells were grown as in (A) and total RNA was isolated with TRIzol. The relative amount of *NFS1* mRNA to *ACT1* mRNA was determined by RT-coupled real-time PCR. Quantifications were performed in quadruplicates and the error bars indicate the standard deviations.
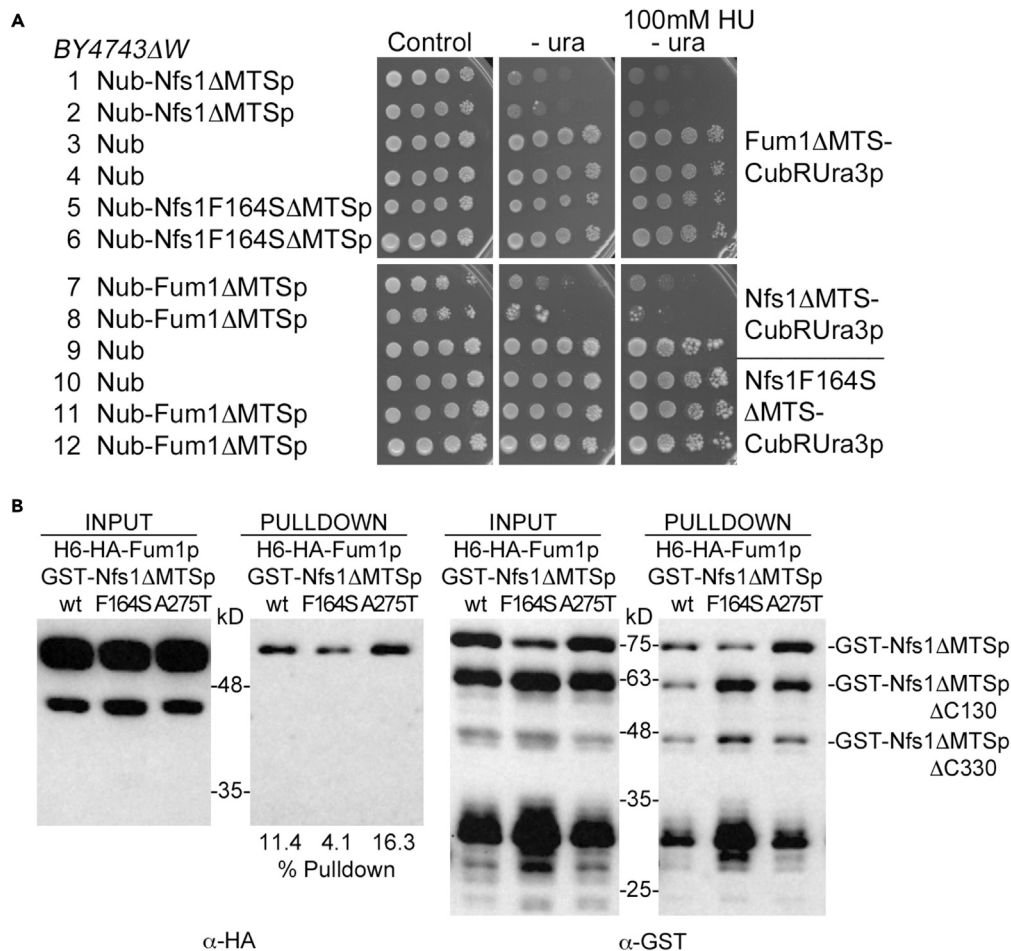
Figure 4. The Nfs1(F164S)p mutant protein is deficient for the protein–protein interaction with fumarase

(A) Nfs1(F164S)p failed to interact with fumarase in the Split-Ub assay in vivo: Cells of the indicated genotype were 10-fold serially diluted, spotted onto the depicted plates, and incubated for six days at 28°C. Protein–protein interactions are indicated by the absence of growth on the plate lacking uracil. Nub-Fum1ΔMTSp was expressed from the *ADH1* promoter, while Nub-Nfs1ΔMTS was expressed from the *NFS1* promoter. Fum1ΔMTS-Cub-RUra3p was expressed from the *FUM1* promoter and Nfs1ΔMTS-Cub-RUra3p was expressed from the *NFS1* promoter.

(B) The interaction between fumarase and Nfs1(F164S)p, but not Nfs1(A275T)p, was reduced in the GST pull-down assays in vitro: The experiment was performed as described in Figure 1D.

isolated *ISU1* and *ISU2* as multi-copy suppressors of the DNA repair defect of the *nfs1S491P* mutant strain (Figure 5A, lines 5 and 6). The overexpression of Isu1/2p also suppressed the DNA repair defect of the *nfs1I492T* mutant strain (Figure 5A, lines 5 and 6). The overexpression of Isu1/2p from the multi-copy plasmid PADNX under the control of the strong *ADH1* promoter also suppressed the HU sensitivity of *nfs1S491P* and *nfs1I492T* (Figure 5B, lines 3 and 5) but not of *nfs1F164S* (Figure S7A, lines 3 and 5). Figure 5B further shows that mitochondrial localization was required for the suppression, as overexpression of Isu1/2p without MTS failed to suppress the DNA repair defect of *nfs1S491P* and *nfs1I492T* (lines 4 and 6). The overexpression of Isu1/2p did not suppress the DNA repair defect of cells lacking fumarase (Figure S7B, lines 11 and 12). The suppression of *nfs1S491P* and *nfs1I492T* by the overexpression of Isu1/2p suggests that the Nfs1(S491P)p and Nfs1(I492T)p mutant proteins may be deficient for the interaction with Isu1/2p, and the split-ubiquitin assay revealed that this was, indeed, the case (Figure 5C; compare line 4 with lines 1, 2, 5, and 6). Consistently, overexpression of Nub-Isu1/2ΔMTSp from the strong *ADH1* promoter restored the protein interaction between the Nfs1(S491P)p mutant protein and Isu1/2p proteins (Figure S7C, lines 5, 6, 11, and 12), while the protein interaction defects of the Nfs1(I492T)p mutant protein were still visible (lines 17, 18, 23, and 24). The structure of human NFS1p and ISCUp is presented in
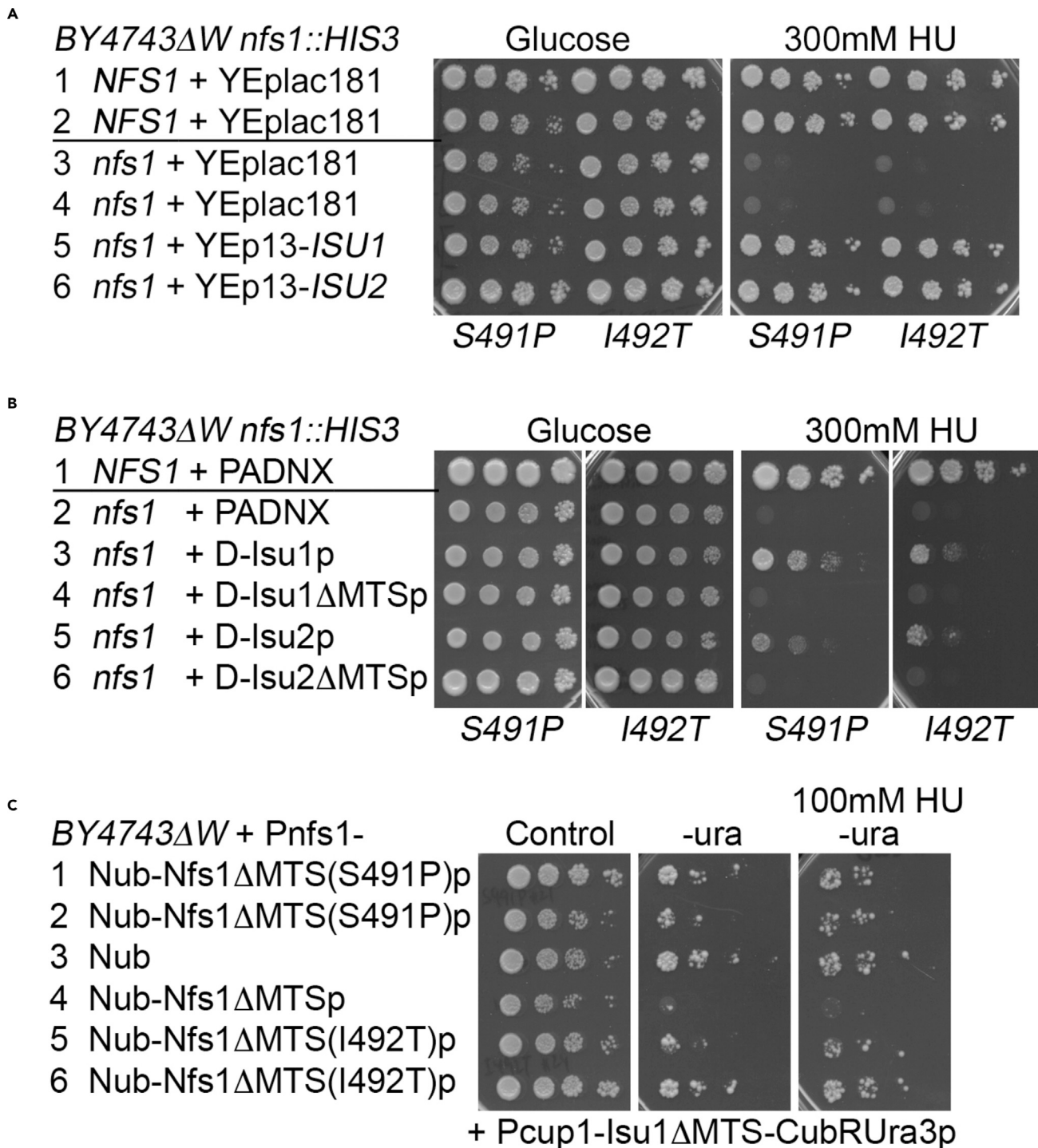
A

BY4743ΔW nfs1::HIS3
1 *NFS1* + YEplac181
2 *NFS1* + YEplac181
3 *nfs1* + YEplac181
4 *nfs1* + YEplac181
5 *nfs1* + YEp13-*ISU1*
6 *nfs1* + YEp13-*ISU2*

B

BY4743ΔW nfs1::HIS3
1 *NFS1* + PADNX
2 *nfs1* + PADNX
3 *nfs1* + D-Isu1p
4 *nfs1* + D-Isu1ΔMTSp
5 *nfs1* + D-Isu2p
6 *nfs1* + D-Isu2ΔMTSp

C

BY4743ΔW + Pnfs1-
1 Nub-Nfs1ΔMTS(S491P)p
2 Nub-Nfs1ΔMTS(S491P)p
3 Nub
4 Nub-Nfs1ΔMTSp
5 Nub-Nfs1ΔMTS(I492T)p
6 Nub-Nfs1ΔMTS(I492T)p

+ Pcup1-Isu1ΔMTS-CubRUra3p

Figure 5. Nfs1S491 and I492 are required for the protein interaction of Nfs1p with Isu1/2p

(A) Overexpression of Isu1/2p from the multi-copy vector YEp13 under the control of their own respective promoters restores DNA repair in *nfs1S491P* and *I492T*: Cells of the indicated genotype were 10-fold serially diluted, spotted onto the depicted plates, and incubated for 12 days at 28°C.

(B) Restoration of DNA repair requires mitochondrial localization of Isu1/2p: Overexpression of Isu1/2p, but not Isu1/2p lacking the mitochondrial targeting signal MTS, from the multi-copy vector PADNX under the control of the strong *ADH1* promoter restored growth of *nfs1S491* and *nfs1I492T* on plates containing 300mM HU: Cells of the indicated genotype were 10-fold serially diluted, spotted onto the depicted plates, and incubated for six days at 28°C.

(C) Nfs1S491 and I492 are required for the protein interaction of Nfs1p with Isu1p: Cells of the indicated genotype were 10-fold serially diluted, spotted onto the depicted plates, and incubated for six days at 28°C. Nub-Nfs1ΔMTSp was expressed from the *NFS1* promoter and Isu1ΔMTS-CubRUra3p was expressed from the *CUP1* promoter. Protein interaction between Nfs1p and Isu1p is revealed by the lack of growth on the plates lacking uracil.

Table 1. N128 and N132 are deamidated predominantly in _Δfum1_ under conditions of DNA damage

Strain	HU	Sequence	No	Modification	%Mod
_BY4743_	–	FYTGLYG**N**PHSNTHSYGWE	19	Deamidated(N128)x1	5
		FYTGLYGNPHS**N**THSYGWE		Deamidated(N132)x1	5
_BY4743_	+	FYTGLYG**N**PHSNTHSYGWE	39	Deamidated(N128)x2	5
		FYTGLYGNPHS**N**THSYGWE		Deamidated(N132)x3	8
Δfum1	–	FYTGLYG**N**PHSNTHSYGWE	26	Deamidated(N128)x2	8
		FYTGLYGNPHS**N**THSYGWE		Deamidated(N132)x2	8
Δfum1	+	FYTGLYG**N**PHSNTHSYGWE	52	Deamidated(N128)x9	17
		FYTGLYGNPHS**N**THSYGWE		Deamidated(N132)x7	13

The table depicts the strains, the growth conditions without (–) and with (+) 400mM HU for two hours, the amino acid sequence with the modified residue in bold, the number of peptides that contained this residue (No), the modification including the number of peptides collected that contained this modification (x) and the percent of peptides with this modification (%Mod). See Table S1 for the total number of Nfs1p peptides collected during MS and the percent coverage of Nfs1p by the peptides collected.

Figure S8. Human NFS1S450 and I451 (which correspond to the positions of S491 and I492 in yeast Nfs1p) interact with ISCUp, the human homolog of yeast Isu1/2p (Boniecki et al., 2017). Thus, we suggest that the _ISU1/ISU2_ dose-dependent suppression of _nfs1S491P_ and _nfs1I492T_ stems from the physical interaction of Isu1/2p with Nfs1p.

Parathymosins that inactivate Nfs1p accumulate in cells lacking fumarase

We initially hypothesized that in wild-type cells, fumarase may prevent succination of the catalytically active C421 of Nfs1p by binding to it and converting any approaching fumarate molecule to malate. Accordingly, in cells, or more specifically, in mitochondria lacking fumarase, fumarate that accumulates owing to the blockage of the TCA cycle, could be used as a substrate to succinate proteins. Worth mentioning is that the amino acid sequence alignment for Nfs1p proteins from 10 different species shows that C421 is completely conserved from yeast to human (Data S1). We expressed a fusion of Nfs1p to the maltose-binding protein (MBP) under the control of the _ACT1_ promoter in _BY4743ΔW_ wild-type and _Δfum1_ cells (Figure S9). We purified the fusion with the help of amylose resin and examined Nfs1p for modifications in the absence and presence of DNA damage by MS. In contrast to our expectation, we found that Nfs1p was not succinated at the catalytically active C421 but rather, 100% of all peptides were carbamidomethylated at C421 (Table S1). Carbamidomethylation occurs during the MS procedure to prevent oxidation of free cysteines. This result demonstrates that the catalytically active Nfs1C421 was not succinated inside the cells as only free cysteines are carbamidomethylated during the MS procedure (Shakir et al., 2017). Although we did not detect succination, we did detect other modifications of Nfs1p following the induction of DNA damage. For the sake of simplicity, these will be described in the next sections according to the position of modified amino acids within the yeast Nfs1p protein sequence (100–200, 200–300, 300–400).

Deamidation of N128 affects the Nfs1p DNA damage response function

Table 1 shows that N128 and N132 were deamidated predominantly in _Δfum1_ cells grown for two hours under conditions of DNA damage. N128 is conserved as N87 in human NFS1p, while N132 is not conserved (Figure 6A). The amino acid sequence alignment for Nfs1p proteins from 10 different species presented as Data S1 shows that N128 is completely conserved from yeast to human, while N132 is conserved as an R in the other nine species. In order to mimic the modifications that had been observed by MS, both N128 and N132 were changed to aspartic acid. Figure 6B shows that both Nfs1p mimics were able to complement the _nfs1_ deletion and sustain growth on a 5-FOA plate (compare _nfs1N128D_ in lines 1 and 2 and _nfs1N132D_ in lines 5 and 6 with the empty vector control in line 3 and wild-type _NFS1_ in line 4). Next, cells expressing both Nfs1p mimics were tested for their ability to support DNA repair. Figure 6C shows that cells expressing Nfs1(N132D)p were able to repair their damaged DNA and grow on the 300mM HU plate, while cells expressing Nfs1(N128D)p were unable to grow in the presence of 300mM HU (compare Nfs1(N128D)p in lines 1 and 2 and Nfs1(N132D)p in lines 5 and 6 with wild-type Nfs1p in lines 3 and 4). Further tests showed that cells expressing Nfs1(N128D)p were also sensitive to 100mM HU, unable to utilize glycerol, and unable to grow at 37°C (Figure S10, lines 1 and 2). Consistent with the results obtained for the other HU-sensitive Nfs1p mutant proteins, Figure 6D shows that Nfs1(N128D)p was expressed at protein levels higher than

A

```
                                                   87
HsNFS1p   57  DVQATTPLDPRVLDAMLPYLINYYGNPHSRTHAYGWESEAAMERARQQVA  115
              D+QATTP DPRVLD ML +     YGNPHS TH+YGWE+  A+E AR   VA
ScNfs1p   98  DMQATTPTDPRVLDTMLKFYTGLYGNPHSNTHSYGWETNTAVENARAHVA  156
                                       128 132
```

B

BY4743ΔW + Pnfs314-

1	N128D	7	N172D
2	N128D	8	N172D
3	-	9	-
4	Nfs1p	10	Nfs1p
5	N132D	11	N173D
6	N132D	12	N173D

nfs1::HIS3 + 33-NFS1

C

BY4743ΔW + Pnfs314-

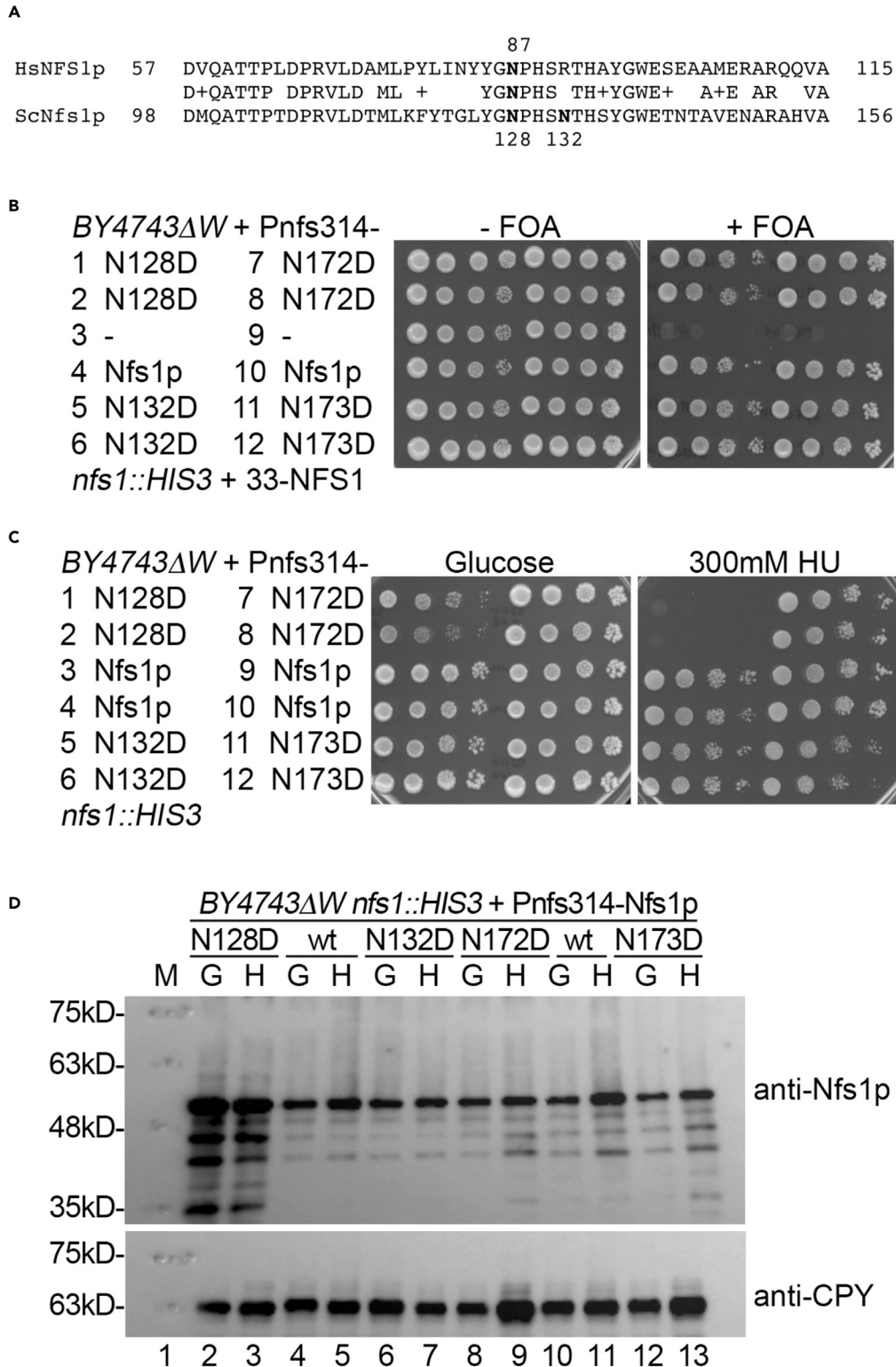|			
1	N128D	7	N172D
2	N128D	8	N172D
3	Nfs1p	9	Nfs1p
4	Nfs1p	10	Nfs1p
5	N132D	11	N173D
6	N132D	12	N173D

nfs1::HIS3

D

Figure 6. Cells expressing Nfs1p deamidated at N128, (but not at N132, N172, or N173) are viable but unable to repair their damaged DNA

Deamidation is mimicked by replacing asparagine with aspartic acid.

(A) Nfs1N128 is conserved as N87 in human NFS1p, while N132 is not conserved. Shown is an alignment between yeast Nfs1p and human NFS1p of the region around Nfs1N128 and N132.

Figure 6. Continued
(B) The ability of the Nfs1p mutant proteins to support viability is revealed by growth on the 5-FOA plate. Cells of the indicated genotype were serially diluted 10fold, spotted onto the depicted plates, and incubated for three days at 28°C.
(C) The ability of the Nfs1p mutant proteins to support DNA repair is revealed by growth on the plate containing 300mM HU. Cells of the indicated genotype were 10-fold serially diluted, spotted onto the depicted plates, and incubated for six days at 28°C.
(D) Cells expressing Nfs1p and its indicated derivatives from the single-copy vector RS314 under the control of the *NFS1* promoter were grown in liquid glucose media in the absence [G] or presence of 400 mM HU for two hours [H]. Cells were boiled in SDS loading dye and proteins were separated on 8%PAA gels. Nfs1p was detected with anti-Nfs1p antibody, while anti-CPY was the loading control.

wild-type Nfs1p (compare lanes 2 and 3 with lanes 4 and 5), while Nfs1(N132D)p was expressed at protein levels comparable to wild-type Nfs1p (compare lanes 4 and 5 with lanes 6 and 7). The same approach was taken for N172 and N173 which were deamidated exclusively in *Δfum1* cells grown for two hours under conditions of DNA damage (Table S2). N172 and N173 are completely conserved from yeast to human (Data S1). In order to mimic the modifications that had been observed by MS, both N172 and N173 were changed to aspartic acid. Figure 6B shows that both Nfs1p mimics were able to complement the *nfs1* deletion and sustain growth on a 5-FOA plate (compare *nfs1N172D* in lines 7 and 8 and *nfs1N173D* in lines 11 and 12 with the empty vector control in line 9 and wild-type *NFS1* in line 10). Figure 6C shows that cells expressing Nfs1(N172D)p were able to repair their damaged DNA and grow on the 300mM HU plate, while cells expressing Nfs1(N173D)p displayed slightly reduced growth in the presence of 300mM HU (compare *nfs1N172D* in lines 7 and 8 and *nfs1N173D* in lines 11 and 12 with *NFS1* wild-type in lines 9 and 10). Thus, we conclude that the deamidations of Nfs1N172 and Nfs1N173 do not significantly affect the Nfs1p function.

Oxidation of M244 affects the Nfs1p DNA damage response function

Table 2 shows that P236 and M244 were modified exclusively in *Δfum1* cells grown for two hours under conditions of DNA damage. P236 was modified to pyro-glutamic acid on 11 out of 42 peptides and M244 was oxidized on 12 out of 42 peptides, with five peptides double-modified. This means that 18 out of the 42 ELEDAIRPDTCLVSVM peptides (=43%) were modified after the cells lacking fumarase had been grown for two hours under conditions of DNA damage. P236 and M244 are conserved as P195 and M203 in human NFS1p (Figure 7A). The amino acid sequence alignment for Nfs1p proteins from 10 different species presented as Data S1 shows that P236 is conserved in 8 out of 10 species, while M244 is conserved in all 10 species. In order to mimic the modifications that had been observed by MS, both P236 and M244 were changed to glutamic acid. Figure 7B shows that both Nfs1p mimics were able to complement the *nfs1* deletion and sustain growth on a 5-FOA plate (compare *nfs1P236E* in lines 1 and 2 and *nfs1M244E* in lines 5 and 6 with the empty vector control in line 3 and wild-type *NFS1* in line 4). Next, cells expressing both Nfs1p mimics were tested for their ability to support DNA repair. Figure 7C shows that cells expressing Nfs1(P236E)p were able to repair their damaged DNA and grow on the 300mM HU plate, while cells expressing Nfs1(M244E)p displayed reduced growth in the presence of 300mM HU (compare *nfs1P236E* in lines 1 and 2 and *nfs1M244E* in lines 5 and 6 with Nfs1p wild-type in lines 3 and 4). Consistently, Nfs1(M244E)p was expressed at higher protein levels as compared to wild-type Nfs1p (Figure 7D, compare lanes 4 and 5 with lanes 6 and 7), while Nfs1(P236E)p was expressed at protein levels comparable to wild-type Nfs1p (compare lanes 2 and 3 with lanes 4 and 5). Further tests showed that cells expressing Nfs1(M244E)p were not sensitive to 100mM HU, able to utilize glycerol, and able to grow at 37°C (Figures S11 and S12). The DNA repair defect of the *nfs1M244E* mutant strain indicates that M244 is required for full Nfs1p function.

N286 and N289 were deamidated exclusively in *Δfum1* cells grown for two hours under conditions of DNA damage (Table S3). In order to mimic the modifications that had been observed by MS, both N286 and N289 were changed to aspartic acid. Figure 7C shows that both Nfs1p mimics were able to complement the *nfs1* deletion with respect to DNA damage sensitivity on HU plates. Thus, we conclude that the deamidations of Nfs1N286 and Nfs1N289 do not affect the Nfs1p function.

Deamidation of Q328 affects the Nfs1p function in cell proliferation

Table 3 shows that Q328 was deamidated predominantly in *Δfum1* cells grown for two hours under conditions of DNA damage. Q328 is conserved as Q287 in human NFS1p (Figure 8A). The amino acid sequence alignment for Nfs1p proteins from 10 different species presented as Data S1 shows that Q328 is completely

Table 2. P236 and M244 are modified exclusively in *Δfum1* cells under conditions of DNA damage

Strain	HU	Sequence	No	Modification	%Mod
BY4743	–	–	0	–	–
BY4743	+	ELEDAIRPDTCLVSVM	2	–	0
Δfum1	–	ELEDAIRPDTCLVSVM	1	–	0
Δfum1	+	ELEDAIR**P**DTCLVSVM	42	Pro- > pyro-Glu(P236)x11	26
		ELEDAIRPDTCLVSV**M**		Oxidation(M244)x12	29
		ELEDAIR**P**DTCLVSV**M**		Double Modified x5	12

The table depicts the strains, the growth conditions without (−) and with (+) 400mM HU for two hours, the amino acid sequence with the modified residue in bold, the number of peptides that contained this residue (No), the modification including the number of peptides collected that contained this modification (x) and the percent of peptides with this modification (%Mod). See Table S1 for the total number of Nfs1p peptides collected during MS and the percent coverage of Nfs1p by the peptides collected.

conserved from yeast to human. In order to mimic the modification that had been observed by MS, Q328 was changed to glutamic acid. Figure 8B shows that the Nfs1p mimic was unable to complement the *nfs1* gene deletion and sustain growth on a 5-FOA plate (compare *nfs1Q328E* in lines 1, 2, 5, and 6 with the empty vector control in line 3 and wild-type *NFS1* in line 4). Figure 8C shows that overexpression of Nfs1(Q328E)p from a multi-copy vector under the control of the strong *ADH1* promoter caused a growth defect and sensitivity to HU in *BY4742ΔW* cells (compare lines 1 and 2 with lanes 3 and 4), presumably by Nfs1(Q328E)p forming hetero-oligomers with wild-type Nfs1p expressed from the chromosome. This dominant-negative effect required mitochondrial localization as cells overexpressing Nfs1(Q328E)p lacking its MTS grew normally (compare lines 3 and 4 with lines 5 and 6). We conclude that Q328 is essential for the function of Nfs1p.

DISCUSSION

The Krebs TCA cycle enzyme fumarase is a metabolic enzyme that converts fumarate to L-malate in the mitochondria of eukaryotes and in the cytoplasm of prokaryotes. In eukaryotic cells, fumarase is dual-localized and a substantial portion of fumarase can be found in the cytosol and nucleus (Yogev et al., 2011; Dik et al., 2016). Fumarase has been identified as a protein involved in the DDR in human, yeast, and bacterial cells (Yogev et al., 2010; Singer et al., 2017; Leshets et al., 2018a; Silas et al., 2021). In eukaryotes upon DNA damage, fumarase enters the nucleus, where it converts L-malate to fumarate as part of the DDR (Yogev et al., 2010). To date, the targets of this fumarase metabolic signaling are elements of the DDR such as histone demethylases in human cells (Jiang et al., 2015; Wang et al., 2017; Saatchi and Kirchmaier, 2019; Sulkowski et al., 2020), Sae2, a DNA resection enzyme in yeast (Leshets et al., 2018b), RecN a protein that triggers DNA repair in *Bacillus subtilis* (Singer et al., 2017), and AlkB, a DNA demethylase in *E. coli* (Silas et al., 2021). Fascinatingly, in all these cases TCA metabolites such as fumarate, L-malate, and α-ketoglutarate transmit the effect of fumarase activity to the respective DDR elements. It is very clear that the activity of fumarase and its associated TCA metabolites are required for the effect on the DDR in the nucleus of eukaryotes.

Here we show that the overexpression of the cysteine desulfurase Nfs1p restores DNA repair in yeast cells lacking fumarase and more importantly that Nfs1p and Fum1p interact both in vivo and in vitro. Both Nfs1p and Fum1p were shown to be dual-targeted to mitochondria and nucleus (Naamati et al., 2009; Yogev et al., 2010). Where does the interaction of Nfs1p and Fum1p occur and where does the Fum1p have to be localized in order to affect the Nfs1p-dependent suppression of the *fum1* deletion? Figures 1B and S1 show that the mitochondrial localization of Nfs1p is required, because cells expressing Nfs1p lacking a targeting signal (ΔMTS) failed to complement the DNA damage sensitivity of cells lacking fumarase. In addition, Nfs1p is "eclipsed distributed" in yeast with the vast majority of the protein in mitochondria and only a minute amount in the nucleus (Naamati et al., 2009). The proposed function of Nfs1p in the nucleus has nothing to do with the DDR (Mühlenhoff et al., 2004). In this regard, Nfs1p provides sulphur and Yfh1p helps the transfer of the S from Nfs1p to Isu1/2p, which, in turn, generates Fe–S clusters in mitochondria (Lill and Freibert, 2020). Yfh1p and Isu1/2p are mitochondrial proteins and in fact, the latter can suppress certain *nfs1* mutations (S491P and I492T) by binding to Nfs1p inside the mitochondria.
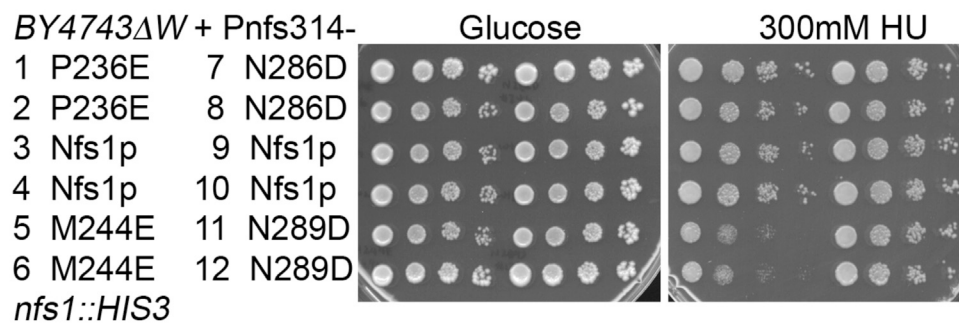
A


```
                              195       203
HsNFS1p 178   VQKSGIIDLKELEAAIQPDTSLVSVMTVNNEIGVKQPIAEIGRICSSRK   226
              V    G+IDLKELE AI+PDT LVSVM VNNEIGV QPI EIG IC    K
ScNfs1p 219   VDDQGLIDLKELEDAIRPDTCLVSVMAVNNEIGVIQPIKEIGAICRKNK   267
                            236       244
```
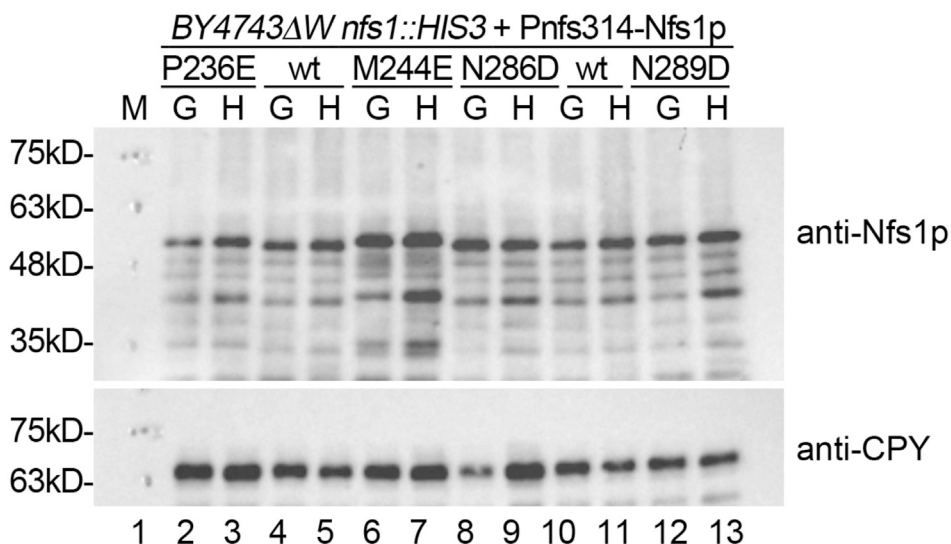
B
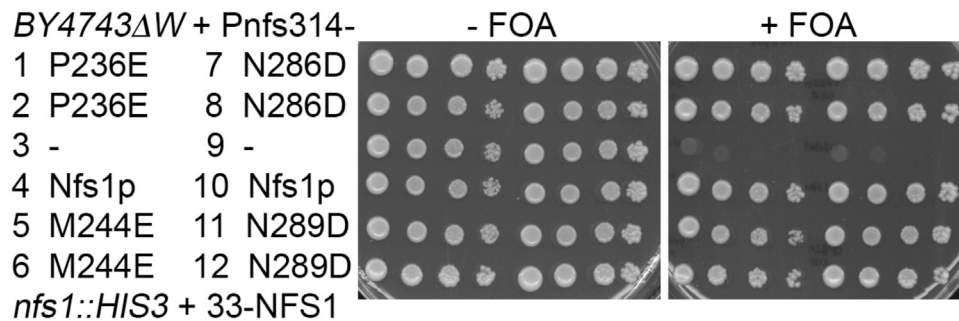
C

D

Figure 7. Cells expressing Nfs1p oxidized at M244 are viable but unable to repair their damaged DNA (while cells expressing Nfs1p with P236 converted to pyro-glutamic acid as well as Nfs1p deamidated at N286 and N289 are viable and able to repair their damaged DNA)

Conversion of P236 to pyro-glutamic acid and oxidation of M244 are mimicked by replacing these residues with glutamic acid, while deamidation is mimicked by replacing asparagine with aspartic acid.

Figure 7. *Continued*

(A) Nfs1P236 is conserved as P195 and M244 is conserved as M203 in human NFS1p. Shown is an alignment between yeast and human Nfs1p of the region around yeast Nfs1P236 and Nfs1M244.

(B) The ability of the Nfs1p mutant proteins to support viability is revealed by growth on the 5-FOA plate. Cells of the indicated genotype were 10-fold serially diluted, spotted onto the depicted plates, and incubated for three days at 28°C.

(C) The ability of the Nfs1p mutant proteins to support DNA repair is revealed by growth on the plate containing 300mM HU. Cells of the indicated genotype were 10-fold serially diluted, spotted onto the depicted plates, and incubated for six days at 28°C.

(D) Cells expressing Nfs1p and its indicated derivatives from the single-copy vector RS314 under the control of the *NFS1* promoter were grown in liquid glucose media in the absence [G] or presence of 400 mM HU for two hours [H]. Cells were boiled in SDS loading dye and proteins were separated on 8%PAA gels. Nfs1p was detected with anti-Nfs1p antibody, while anti-CPY was the loading control.

Fe–S clusters are important co-factors for DNA repair enzymes (see the Introduction), and our results indicate that active Nfs1p becomes limiting in cells lacking fumarase. We hypothesize that under fumarase depletion, lack of respiration, and oxidizing conditions in mitochondria cause Nfs1p to spontaneously accumulate inactivating modifications. In this regard, the Nfs1 C421 in the enzyme's catalytically active site is not modified; nevertheless, we detected numerous modifications of other amino acids of Nfs1p. It is important to emphasize that all these modifications are unlikely to be mediated by some protein-modifying enzyme, but rather, they are spontaneous modifications that occur under oxidizing conditions. In order to detect Nfs1p inactivating modifications, we tested mimics of these modifications for their ability to support viability and DNA repair. We have found that Nfs1p accumulates inactivating modifications at N128, M244, and Q328 in cells lacking fumarase. N128 was deamidated in 17.3% (9/52) of peptides in cells lacking fumarase and in 5.1% (2/39) of peptides in wild-type cells. M244 was oxidized in 28.6% (12/42) of peptides in cells lacking fumarase and in 0% (0/2) of peptides in wild-type cells. Q328 was deamidated in 9.0% (7/78) of peptides in cells lacking fumarase and in 1.3% (1/78) of peptides in wild-type cells. Under the assumption that the inactivating modifications occur independently on separate protein molecules, we estimate that under conditions of DNA damage, when Fe–S clusters are required for the DNA repair enzymes to repair the damaged DNA, approximately half of the Nfs1p molecules were inactivated by these modifications in cells lacking fumarase, while only some 6% of Nfs1p molecules were inactivated in wild-type cells. This means that active Nfs1p becomes limiting in *Δfum1* cells, which explains why the overexpression of Nfs1p was able to restore DNA repair in cells lacking fumarase. Our model is that in addition to metabolic signaling of the DDR in the nucleus, fumarase affects the DDR by protecting the desulfurase Nfs1p in mitochondria from modification and inactivation. Fumarase performs this protection in two respects (i) directly binding to Nfs1p in mitochondria and (ii) enabling, the maintenance, via metabolism, of a non-oxidizing environment in mitochondria.

Limitations of the study

In this study, we reveal a novel way by which fumarase is involved in DNA repair. This is not directly by the enzyme or one of its metabolites interacting with a DNA repair factor, as previously described for eukaryotes and prokaryotes. In this case, fumarase protects the mitochondrial cysteine desulfurase Nfs1p from modification and inactivation, which in turn indirectly can affect DNA repair enzymes such as DNA polymerase and Xeroderma Pigmentosum group D (XPD) which require Fe–S cofactors to function. We have used aconitase as a proxy to show that Fe–S clusters are limiting in Nfs1-deficient yeast cells; however, we have

Table 3. Q328 is predominantly deamidated in *Δfum1* cells under conditions of DNA damage.

Strain	HU	Sequence	No	Modification	%Mod
BY4743	–	LEPLLSGGG**Q**ERGLRSGTL	59	Deamidated(Q328)x1	2
BY4743	+	LEPLLSGGG**Q**ERGLRSGTL	78	Deamidated(Q328)x1	1
Δfum1	–	LEPLLSGGG**Q**ERGLRSGTL	88	Deamidated(Q328)x2	2
Δfum1	+	LEPLLSGGG**Q**ERGLRSGTL	78	Deamidated(Q328)x7	9

The table depicts the strains, the growth conditions without (–) and with (+) 400mM HU for two hours, the amino acid sequence with the modified residue in bold, the number of peptides that contained this residue (No), the modification including the number of peptides collected that contained this modification (x) and the percent of peptides with this modification (%Mod). See Table S1 for the total number of Nfs1p peptides collected during MS and the percent coverage of Nfs1p by the peptides collected.
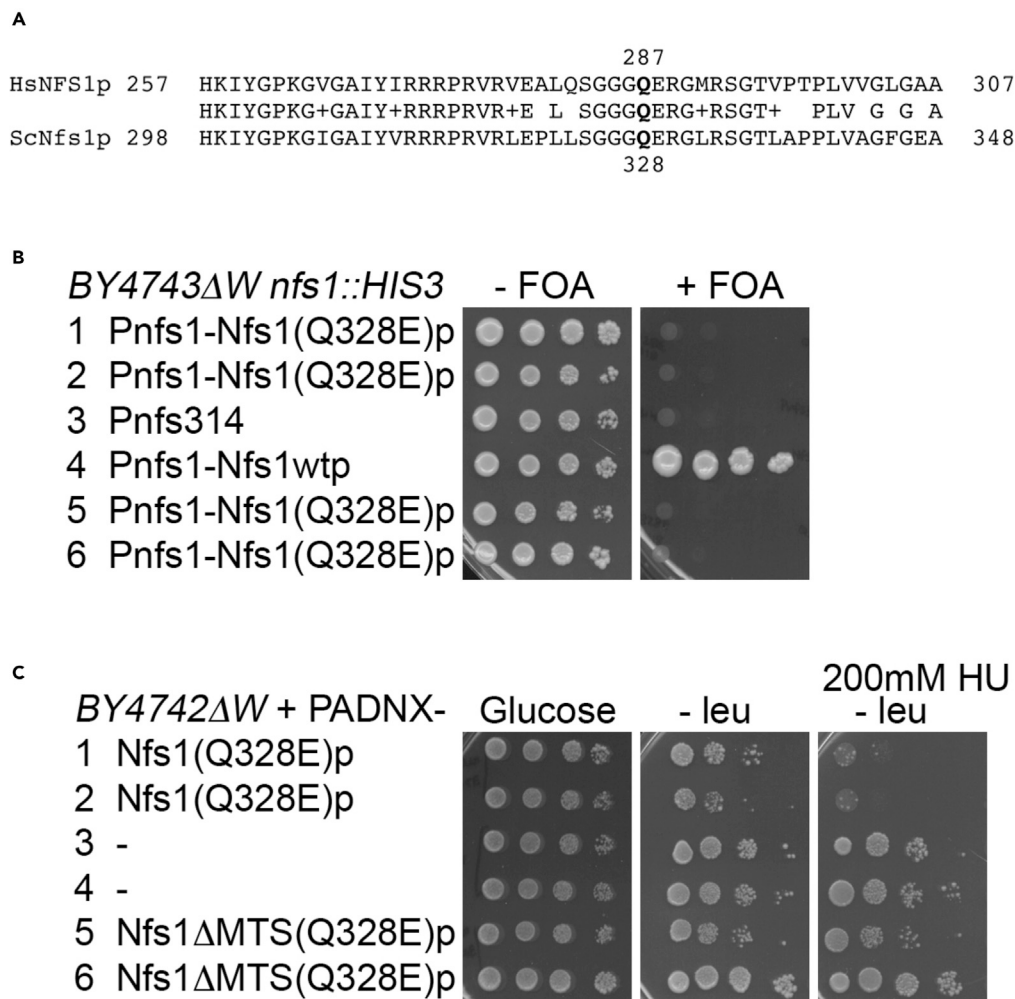
A

```
                                                  287
HsNFS1p 257   HKIYGPKGVGAIYIRRRPRVRVEALQSGGGQERGMRSGTVPTPLVVGLGAA   307
              HKIYGPKG+GAIY+RRRPRVR+E L SGGGQERG+RSGT+  PLV G G A
ScNfs1p 298   HKIYGPKGIGAIYVRRRPRVRLEPLLSGGGQERGLRSGTLAPPLVAGFGEA   348
                                                  328
```

B

C

Figure 8. Nfs1p function requires Q328

Deamidation is mimicked by replacing Q328 with E

(A) Nfs1Q328 is conserved as Q287 in human NFS1p. Shown in an alignment between yeast Nfs1p and human NFS1p of the region around Nfs1Q328.

(B) The Nfs1(Q328E)p mutant protein is unable to support viability, which is revealed by the absence of growth on the 5-FOA plate: Cells of the indicated genotype were 10-fold serially diluted, spotted onto the depicted plates, and incubated at 28°C for three days on the plate without 5-FOA and for 12 days on the plate with 5-FOA.

(C) Nfs1(Q328E)p overexpressed from the multi-copy vector PADNX under the control of the strong *ADH1* promoter is dominant-negative: Cells of the indicated genotype were 10-fold serially diluted, spotted onto the depicted plates, and incubated for six days at 28°C.

not demonstrated that DNA polymerase and XPD are the targets of this shortage in Fe–S clusters. Thus, one understanding is we have probably not discovered all the targets, roles, metabolic pathways, in which fumarase aids DNA repair. Furthermore, we have not shown that Fe–S clusters are, indeed, limiting in fumarase-deficient human cells and that Fe–S clusters could be used to treat patients with HLRCC.

STAR★METHODS

Detailed methods are provided in the online version of this paper and include the following:

- KEY RESOURCES TABLE
- RESOURCE AVAILABILITY
  - Lead contact
  - Materials availability

SUPPLEMENTAL INFORMATION

Supplemental information can be found online at https://doi.org/10.1016/j.isci.2021.103354.

AUTHOR CONTRIBUTIONS

JY contributed Figures 1, 2, and 4; SW contributed Figures 3, 5, 6, 7, and 8; JT helped JY and SQ; TKL and QL performed the MS; ZY and OK performed the subcellular fractionation; OP and NL designed the experiments, wrote the manuscript and supervised JY, SW, and ZY.

DECLARATION OF INTERESTS

NL is co-owner of a patent covering the split-ubiquitin system [US patent no 20040170970. Varshavsky A, Wittke S, Johnsson N and Lehming N (2004) split-ubiquitin based reporter systems and methods of their use].

REFERENCES

Adam, A.C., Bornhövd, C., Prokisch, H., Neupert, W., and Hell, K. (2006). The Nfs1 interacting protein Isd11 has an essential role in Fe/S cluster biogenesis in mitochondria. EMBO J. 25, 174–183.

Alani, E., Cao, L., and Kleckner, N. (1987). A method for gene disruption that allows repeated use of URA3 selection in the construction of multiply disrupted yeast strains. Genetics 116, 541–545.

Alvarez, S.W., Sviderskiy, V.O., Terzi, E.M., Papagiannakopoulos, T., Moreira, A.L., Adams, S., Sabatini, D.M., Birsoy, K., and Possemato, R. (2017). NFS1 undergoes positive selection in lung tumours and protects cells from ferroptosis. Nature 55, 639–643.

Barros, M.H., and McStay, G.P. (2020). Modular biogenesis of mitochondrial respiratory complexes. Mitochondrion 50, 94–114.

Bedekovics, T., Li, H., Gajdos, G.B., and Isaya, G. (2011). Leucine biosynthesis regulates cytoplasmic iron-sulfur enzyme biogenesis in an

Atm1p-independent manner. J. Biol. Chem. 286, 40878–40888.

Blatnik, M., Thorpe, S.R., and Baynes, J.W. (2008). Succination of proteins by fumarate: mechanism of inactivation of glyceraldehyde-3-phosphate dehydrogenase in diabetes. Ann. N. Y. Acad. Sci. 1126, 272–275.

Boniecki, M.T., Freibert, S.A., Mühlenhoff, U., Lill, R., and Cygler, M. (2017). Structure and functional dynamics of the mitochondrial Fe/S cluster synthesis complex. Nat. Commun. 8, 1287.

Cardenas-Rodriguez, M., Chatzi, A., and Tokatlidis, K. (2018). Iron–sulfur clusters: from metals through mitochondria biogenesis to disease. J. Biol. Inorg. Chem. 23, 509–520.

Chew, B.S., Siew, W.L., Xiao, B., and Lehming, N. (2010). Transcriptional activation requires protection of the TATA-binding protein Tbp1 by the ubiquitin-specific protease Ubp3. Biochem. J. 431, 391–399.

Coelho, M.C., Pinto, R.M., and Murray, A.W. (2019). Heterozygous mutations cause genetic

instability in a yeast model of cancer evolution. Nature 566, 275–278.

Daum, G., Böhni, P.C., and Schatz, G. (1982). Import of proteins into mitochondria. Cytochrome b2 and cytochrome c peroxidase are located in the intermembrane space of yeast mitochondria. J. Bio. Chem. 257, 13028–13033.

Dik, E., Naamati, A., Asraf, H., Lehming, N., and Pines, O. (2016). Human fumarate hydratase is dual localized by an alternative transcription initiation mechanism. Traffic 17, 720–732.

Fuss, J.O., Tsai, C.L., Ishida, J.P., and Tainer, J.A. (2015). Emerging critical roles of Fe-S clusters in DNA replication and repair. Biochim. Biophys. Acta 1853, 1253–1271.

Gietz, R.D., and Sugino, A. (1988). New yeast-Escherichia coli shuttle vectors constructed with in vitro mutagenized yeast genes lacking six-base pair restriction sites. Gene 74, 527–534.

Hanahan, D., and Weinberg, R.A. (2011). Hallmarks of cancer: the next generation. Cell 144, 646–674.

Jiang, Y., Qian, X., Shen, J., Wang, Y., Li, X., Liu, R., Xia, Y., Chen, Q., Peng, G., Lin, S.Y., and Lu, Z. (2015). Local generation of fumarate promotes DNA repair through inhibition of histone H3 demethylation. Nat. Cell Biol. *17*, 1158–1168.

Krebs, H.A., Salvin, E., and Johnson, W.A. (1938). The formation of citric and alpha-ketoglutaric acids in the mammalian body. Biochem. J. *32*, 113–117.

Kispal, G., Csere, P., Prohl, C., and Lill, R. (1999). The mitochondrial proteins Atm1p and Nfs1p are essential for biogenesis of cytosolic Fe/S proteins. EMBO J. *18*, 3981–3989.

Laser, H., Bongards, C., Schüller, J., Heck, S., Johnsson, N., and Lehming, N. (2000). A new screen for protein interactions reveals that the Saccharomyces cerevisiae high mobility group proteins Nhp6A/B are involved in the regulation of the GAL1 promoter. Proc. Natl. Acad. Sci. U S A *97*, 13732–13737.

Lehming, N. (2002). Analysis of protein-protein proximities using the split-ubiquitin system. Brief. Funct. Genomic Proteomic. *1*, 230–238.

Leshets, M., Silas, Y.B.H., Lehming, N., and Pines, O. (2018a). Fumarase: from the TCA cycle to DNA damage response and tumor suppression. Front Mol. Biosci. *5*, 68.

Leshets, M., Ramamurthy, D., Lisby, M., Lehming, N., and Pines, O. (2018b). Fumarase is involved in DNA double-strand break resection through a functional interaction with Sae2. Curr. Genet. *64*, 697–712.

Lill, R., and Freibert, S.A. (2020). Mechanisms of mitochondrial iron-sulfur protein biogenesis. Annu. Rev. Biochem. *89*, 471–499.

Lim, M.K., Tang, V., Le Saux, A., Schüller, J., Bongards, C., and Lehming, N. (2007). Gal11p dosage-compensates transcriptional activator deletions via Taf14p. J. Mol. Biol. *374*, 9–23.

Mühlenhoff, U., Balk, J., Richhardt, N., Kaiser, J.T., Sipos, K., Kispal, G., and Lill, R. (2004). Functional characterization of the eukaryotic cysteine desulfurase Nfs1p from Saccharomyces cerevisiae. J. Biol. Chem. *279*, 36906–36915.

Naamati, A., Regev-Rudzki, N., Galperin, S., Lill, R., and Pines, O. (2009). Dual targeting of Nfs1 and discovery of its novel processing enzyme, Icp55. J. Biol. Chem. *284*, 30200–30208.

Nasmyth, K.A., and Reed, S.I. (1980). Isolation of genes by complementation in yeast: molecular cloning of a cell-cycle gene. Proc. Natl. Acad. Sci. USA *77*, 2119–2123.

Netz, D.J., Stith, C.M., Stümpfig, M., Köpf, G., Vogel, D., Genau, H.M., Stodola, J.L., Lill, R., Burgers, P.M., and Pierik, A.J. (2011). Eukaryotic DNA polymerases require an iron-sulfur cluster for the formation of active complexes. Nat. Chem. Biol. *8*, 125–132.

Saatchi, F., and Kirchmaier, A.L. (2019). Tolerance of DNA replication stress is promoted by fumarate through modulation of histone demethylation and enhancement of replicative intermediate processing in saccharomyces cerevisiae. Genetics *212*, 631–654.

Shakir, S., Vinh, J., and Chiappetta, G. (2017). Quantitative analysis of the cysteine redoxome by iodoacetyl tandem mass tags. Anal. Bioanal. Chem. *409*, 3821–3830.

Sikorski, R.S., and Hieter, P. (1989). A system of shuttle vectors and yeast host strains designed for efficient manipulation of DNA in Saccharomyces cerevisiae. Genetics *122*, 19–27.

Singer, E., Silas, Y.B., Ben-Yehuda, S., and Pines, O. (2017). Bacterial fumarase and L-malic acid are evolutionary ancient components of the DNA damage response. Elife *6*, e30927.

Silas, Y., Singer, E., Lehming, N., and Pines, O. (2021). A combination of class-I fumarases and

metabolites (α-ketoglutarate and fumarate) signal the DNA damage response in Escherichia coli. Proc. Natl. Acad. Sci. U S A *118*. e2026595118. https://doi.org/10.1073/pnas.2026595118.

Sulkowski, P.L., Oeck, S., Dow, J., Economos, N.G., Mirfakhraie, L., Liu, Y., Noronha, K., Bao, X., Li, J., Shuch, B.M., et al. (2020). Oncometabolites suppress DNA repair by disrupting local chromatin signalling. Nature *582*, 586–591.

Tomlinson, I.P., Alam, N.A., Rowan, A.J., Barclay, E., Jaeger, E.E., Kelsell, D., Leigh, I., Gorman, P., Lamlum, H., Rahman, S., et al. (2002). Germline mutations in FH predispose to dominantly inherited uterine fibroids, skin leiomyomata and papillary renal cell cancer. Nat. Genet. *30*, 406–410.

Wang, T., Yu, Q., Li, J., Hu, B., Zhao, Q., Ma, C., Huang, W., Zhuo, L., Fang, H., Liao, L., et al. (2017). O-GlcNAcylation of fumarase maintains tumour growth under glucose deficiency. Nat. Cell Biol. *19*, 833–843.

Wang, S., Ramamurthy, D., Tan, J., Liu, J., Yip, J., Chua, A., Yu, Z., Lim, T.K., Lin, Q., Pines, O., and Lehming, N. (2020). Post-translational modifications of fumarase regulate its enzyme activity and function in respiration and the DNA damage response. J. Mol. Biol. *432*, 6108–6126.

Yang, M., Ternette, N., Su, H., Dabiri, R., Kessler, B.M., Adam, J., Teh, B.T., and Pollard, P.J. (2014). The succinated proteome of FH-mutant tumours. Metabolites *4*, 640–654.

Yogev, O., Naamati, A., and Pines, O. (2011). Fumarase: a paradigm of dual targeting and dual localized functions. FEBS J. *278*, 4230–4242.

Yogev, O., Yogev, O., Singer, E., Shaulian, E., Goldberg, M., Fox, T.D., and Pines, O. (2010). Fumarase: a mitochondrial metabolic enzyme and a cytosolic/nuclear component of the DNA damage response. Plos Biol. *8*, e1000328.

STAR★METHODS

KEY RESOURCES TABLE

REAGENT or RESOURCE	SOURCE	IDENTIFIER
Antibodies		
Mouse monoclonal anti-CPY	Invitrogen	Cat#A6428; 10A5
Mouse monoclonal anti-GST	Novagen	Cat#71097; D00166705
Mouse monoclonal anti-HA	Roche	Cat#11583816001; 12CA5
Mouse monoclonal anti-MBP	NEB	Cat#E8032L; B48
Rabbit polyclonal anti-Nfs1	Ophry Pines	Naamati et al., 2009
Goat anti-Mouse-HRP	Bio-Rad	Cat#1706516
Goat anti-Rabbit-HRP	Bio-Rad	Cat#1662408
Bacterial and virus strains		
DH5α	ThermoFisher	Cat#18265017
BL21LysS	ThermoFisher	Cat#C602003
Biological samples		
NIL		
Chemicals, peptides, and recombinant proteins		
5-Fluoroorotic acid (FOA)	BioVectra	Cat#1556
Hydroxyurea (HU)	US Biological Life Sciences	Cat#H9120
Critical commercial assays		
ECL	GE Healthcare (Amersham)	RPN2232 (prime) RPN2235 (select)
Deposited data		
https://data.mendeley.com/datasets/29m8fjsjd4/draft?a=8f5af9cd-b266-4c5d-8362-1bfe368dd711	Norbert Lehming	
Experimental models: Organisms/strains		
BY4741	EUROSCARF	Cat#Y00000
BY4741ΔW	Norbert Lehming	Lim et al., 2007
BY4741ΔWΔfum1	Norbert Lehming	Wang et al., 2020
BY4742	EUROSCARF	Cat#Y10000
BY4742ΔW	Norbert Lehming	Lim et al., 2007
BY4742ΔWΔfum1	Norbert Lehming	Wang et al., 2020
BY4743	EUROSCARF	Cat#Y20000
BY4743ΔW	Norbert Lehming	Lim et al., 2007
BY4743ΔWΔfum1	Norbert Lehming	Wang et al., 2020
The *Saccharomyces cerevisiae* strains generated for this study are listed in Table S4	Norbert Lehming	This study
Oligonucleotides		
5ACT1+1132: GACCAAACTACTTACAACTCCA (qPCR)	Axil Scientific	This study
3ACT1-1248: CATTCTTTCGGCAATACCTG (qPCR)	Axil Scientific	This study
5NFS+1067: TTGACAACGACCAAGCTCAC (qPCR)	Axil Scientific	This study
3NFS1-1261: AGGCTGAACCCGAGGATAAT (qPCR)	Axil Scientific	This study
The primers used for molecular cloning are listed in Table S5	Axil Scientific	This study
Recombinant DNA		
Multi-copy library of *Saccharomyces cerevisiae* genomic DNA fragments in YEp13	ATCC	Cat#37323
Nub fusion library of *Saccharomyces cerevisiae* genomic DNA fragments	Norbert Lehming	Laser et al., 2000

Continued

REAGENT or RESOURCE	SOURCE	IDENTIFIER
pET11a	Novagen	Cat#69436
pET11a-H6HA-Fum1ΔMTS	Norbert Lehming	This study
pGEX-5X-1	Amersham	Cat#28954553
pGEX-5X-1-Nfs1ΔMTS	Norbert Lehming	This study
YCplac33	ATCC	Cat#87586
YCplac33-NFS1	Norbert Lehming	This study
puc8+HIS3	Norbert Lehming	Chew et al., 2010
puc8+HIS3-PTnfs1	Norbert Lehming	This study
pRS314	ATCC	Cat#77143
Pnfs314-Nfs1p	Norbert Lehming	This study
PactT314	Norbert Lehming	Wang et al., 2020
PactT314-Nfs1p	Norbert Lehming	This study
pRS424	ATCC	Cat#77105
PactT424	Norbert Lehming	Wang et al., 2020
PactT424-MBP	Norbert Lehming	This study
Software and algorithms		
Image Lab	Bio-Rad	6.0.1
Other		
Amylose Resin	NEB	Cat#E8021S
Glutathione Sepharose	Amersham	Cat#17513202

RESOURCE AVAILABILITY

Lead contact

Further information and requests for resources and reagents should be directed to and will be fulfilled by the lead contact, Norbert Lehming (micln@nus.edu.sg).

Materials availability

Yeast strains and plasmids generated in this study are available upon request without restrictions.

Data and code availability

- The original data of the figures presented in this study are available at https://data.mendeley.com/datasets/29m8fjsjd4/draft?a=8f5af9cd-b266-4c5d-8362-1bfe368dd711

- This paper does not report original code.

- Any additional information required to reanalyze the data reported in this paper is available from the lead contact upon request.

EXPERIMENTAL MODEL AND SUBJECT DETAILS

Strains, libraries, plasmids and antibodies

BY4741ΔW and *BY4742ΔW* and their gene deletion derivative strains were generated from the parental strains that had been obtained from EUROSCARF. *TRP1* knockout was achieved through insertion of *hisG* with the help of *NKY1009* (Alani et al., 1987). *BY4743ΔW* and the gene deletion derivatives were generated by mating the respective *BY4741ΔW* and *BY4742ΔW* strains and plating on plates lacking both methionine and lysine. A complete list of strains used in the study is listed in Table S4. The multi-copy library of *S. cerevisiae* genomic DNA fragments (Nasmyth and Reed, 1980) and the Nub fusion library of *S. cerevisiae* genomic DNA fragments (Laser et al., 2000) have been described previously. H6-HA-Fum1ΔMTSp was expressed from pET11a (Novagen) and GST-Nfs1ΔMTSp was expressed from pGEX-5X-1 (Amersham). In order to delete the essential *NFS1* gene from chromosome III, the entire *NFS1* gene (including some 500 bp of promoter and terminator) was

cloned into the *URA3*-marked plasmid YCplac33 (Gietz and Sugino, 1988) and transformed into *BY4741ΔW* and *BY4742ΔW*. Next, the chromosomal *NFS1* genes were replaced by *HIS3* on plates lacking histidine with the help of *EcoRI/SalI* cut puc8+HIS3-PTnfs1, which contains some 500 bp of *NFS1* promoter and terminator flanking the *HIS3* gene. The two haploid strains were mated to obtain the diploid *NFS1* gene deletion strain *BY4743ΔW nfs1::HIS3* + YCplac33-NFS1. In order to obtain the HU-sensitive *nfs1* mutant strains, the entire *NFS1* gene including some 500 bp of promoter and terminator was mutagenized by PCR with *Taq* DNA polymerase and gap-repaired into Pnfs314, which contains some 500 bp of *NFS1* promoter and terminator cloned into pRS314 (Sikorski and Hieter, 1989). Transformants on 5-FOA plates lacking tryptophan were replica-plated onto plates with and without 300mM HU. Plasmids of colonies unable to grow on the HU plates were isolated from the replica plate without HU and tested for plasmid linkage of the HU-sensitivity phenotype. The mutations of the *NFS1* genes of confirmed plasmids were determined by DNA sequencing. *NFS1* genes that contained more than one mutation were sub-cloned in order to determine the functionally relevant mutation. The *TRP1*-marked multi-copy vector PactT424-MBP expressing MBP fusions from the *ACT1* promoter/terminator cassette was generated by amplifying MBP with the primers listed in Table S2 and cloning it into PactT424 (Wang et al., 2020). The mutations mimicking the observed PTMs were generated by sequential PCR with the primers listed in Table S5. The rabbit polyclonal anti-Nfs1p antibody has been described previously (Naamati et al., 2009). The mouse monoclonal anti-CPY antibody is from Invitrogen (10A5), the mouse monoclonal anti-GST antibody is from Novagen (D00166705), the mouse monoclonal anti-HA antibody is from Roche (12CA5) and the mouse monoclonal anti-MBP antibody is from New England Biolabs (B48). Secondary goat anti-mouse (Cat#1706516) and goat anti-rabbit (Cat#1662408) IgG horseradish peroxidase conjugated antibodies are from BIO RAD. Protein bands were visualized with ECL (Amersham), documented with a ChemiDoc XRS+ (Bio-Rad) and quantified with Image Lab 6.0.1 (Bio-Rad).

METHOD DETAILS

Subcellular fractionation

Yeast cells grown to logarithmic phase were harvested and subjected to subcellular fractionations as described previously (Daum et al., 1982) with some modifications. Spheroplasts were prepared in the presence of 20T (MP Biomedicals, Irvine, CA). 3 mL of homogenization buffer (0.6 M sorbitol, 20 mM HEPES, pH7.5) supplemented with 1x Protease Inhibitor Cocktail (P8215, Sigma) and 0.5 mM PMSF was applied to spheroplasts prepared from 100 OD600 units of cells for homogenization. The homogenized spheroplasts cleared of cell debris by subsequent 1,500 g centrifugation for 6 min are defined as total fractions. 10,000 g centrifugation for 10 min was used to separate mitochondria from the total fractions. The postmitochondrial supernatant and the isolated mitochondria, which were resuspended after washing (once) are defined as cytosolic and mitochondrial fractions, respectively.

Split-Ubiquitin screen

The Split-Ubiquitin system for identifying protein-protein interactions is based upon the reconstitution of ubiquitin (Lehming, 2002). Two interacting proteins are fused to the N- and to the C-terminal halves of ubiquitin (Nub and Cub), respectively. Cub is extended by a modified Ura3p enzyme carrying an arginine as first amino acid (RUra3p). The protein-protein interaction reconstitutes ubiquitin, the ubiquitin-specific proteases cleave the C-terminal fusion protein and expose the arginine of RUra3p to the N-end rule protein degradation pathway. As a consequence, cells expressing pairs of interacting proteins become resistant to the drug 5-fluoroorotic acid (FOA) and can be positively selected. The library of *S. cerevisiae* genomic DNA fragments fused to Nub has been described previously (Laser et al., 2000).

GST pull-down assay

H_6-HA-Fum1ΔMTSp, GST and GST-Nfs1ΔMTSp were expressed in *BL21LysS E. coli* cells. Cells were lysed by freeze/thaw in the presence of DNase and protein extracts were generated by centrifugation. Equal amounts of GST and GST-Nfs1ΔMTSp protein extracts were mixed with equal amounts of H_6-HA-Fum1ΔMTSp. GST and GST-Nfs1ΔMTSp were purified with the help of glutathione sepharose (Amersham). Proteins were eluted from the sepharose with SDS loading dye and separated on 8% PAA gels. Proteins were blotted onto Nitrocellulose membranes and input and pull-down were detected with the help of anti-GST and anti-HA antibodies.

mRNA quantification

S. cerevisiae cells were cultured in synthetic complete 2% (w/v) glucose medium at 28°C. At $OD_{600\,nm}$ = 1, the cells were collected by centrifugation. Total RNA was isolated using TRIzol according to the manufacturer's

protocol. cDNA was generated by reverse transcription PCR using TaqMan MicroRNA Reverse Transcription Kit (Roche Applied Biosystems). Quantitative real-time PCR was performed using SYBR Green PCR Master Mix (Applied Biosystems). Primers used for *NFS1* mRNA were 5′-ttgacaacgaccaagctcac-3′ and 5′-aggctgaaccc-gaggataat-3′, and primers used for *ACT1* mRNA were 5′-gaccaaactacttacaactcca-3′ and 5′-cattctttcggcaa-tacctg-3′. All mRNA quantifications were performed in quadruplicate, and the error bars represent the standard deviations.

Mass spectrometry

BY4743ΔW and *BY4743ΔWΔfum1* cells expressing MBP-Nfs1p from the strong *ACT1* promoter were grown in 50 mL liquid glucose media at 28°C to OD_{600nm} = 1. For conditions of DNA damage [H], 400mM HU was added to the cultures and incubation was continued for an additional two hours. For normal conditions [G], incubation was continued for additional one hour. Cell extracts were prepared with glass beads, MBP-Nfs1p was purified with the help of amylose resin (NEB) and eluted from the beads with SDS loading dye. Proteins were separated on 8% PAA gels and detected with an anti-MBP antibody while an anti-CPY antibody served as loading control. Protein bands corresponding to the size of MBP-Nfs1p were excised from the polyacrylamide gel stained with Coomassie Blue and in-gel trypsinated. The tryptic peptides were subjected to liquid chromatography – mass spectrometry (LC-MS) analysis using an Eksigent NanoLC Ultra and cHiPLC-nanoflex (Eksigent) in trap-elute configuration, with a 200 μm × 0.5 mm trap column and a 75 μm × 150 mm analytical column. Both trap and analytical columns were made of ChromXP C18-CL, 3 μm (Eksigent). Peptides were separated by a gradient formed by 2% ACN, 0.1% FA (mobile phase A) and 98% ACN, 0.1% FA (mobile phase B): 5%–7% of mobile phase B in 0.1 min, 7%–30% of mobile phase B in 10 min, 30%–60% of mobile phase B in 4min, 60%–90% of mobile phase B in 1 min, 90%–90% of mobile phase B in 5 min, 90%–5% of mobile phase B in 1 min and 5%–5% of mobile phase B in 10 min, at a flow rate of 300 nL/min. The MS analysis was performed on a TripleTOF 5600 system (AB SCIEX, Foster City, CA, USA) in Information Dependent Mode. MS spectra were acquired across the mass range of 400–1250 m/z in high resolution mode (>30,000) using 250 ms accumulation time per spectrum. A maximum of 10 precursors per cycle were chosen for fragmentation from each MS spectrum with 100 ms minimum accumulation time for each precursor and dynamic exclusion for 8 s. Tandem mass spectra were recorded in high sensitivity mode (resolution >15,000) with rolling collision energy on. Peptide identification and the detection of post-translational modifications were carried out with the ProteinPilot 5.0 software Revision 4769 (AB SCIEX) using the Paragon database search algorithm (5.0.0.0.4767), against a protein sequence database (6723 entries) of the yeast *Saccharomyces cerevisiae*.